

UTILISATION OF NATURAL HYDROXYAPATITE FROM LATES CALCARIFER SCALES TO INCREASE THE BIOACTIVITY IN SS 316L WITH THE DIP COATING METHOD FOR BONE IMPLANTS

NURFITRI RAHMI SARI*, RIZA VERDIAN*, IQBAL YUNANDA PUTRA*, JON AFFI*, ADE INDRA**, IS PRIMA NANDA*, #GUNAWARMAN*

*Department of Mechanical Engineering, Universitas Andalas, Padang, Indonesia

**Department of Mechanical Engineering, Institut Teknologi Padang, Padang, Indonesia

#E-mail: gunawarman@eng.unand.ac.id

Submitted May 25, 2023; accepted June 29, 2023

Keywords: SS 316L, Hydroxyapatite, *Lates Calcarifer* Scales, Dip Coating, Withdrawal Speed

Hydroxyapatite (HA) from Lates Calcarifer scales was used as a coating material for 316L Stainless Steel (SS 316L) to determine the influence of the thickness and withdrawal speed on the morphology of the layer. The dip coating method was used with variations in the mass of the HA in the coating suspension at a constant immersion time and carried out at 2 withdrawal speeds. The withdrawal speed used was $2 \text{ mm}\cdot\text{s}^{-1}$ and $4 \text{ mm}\cdot\text{s}^{-1}$ with variations in the HA content in the suspension of 4 g, 8 g, and 12 g at a constant immersion time of 10 seconds. Analysis of morphological characteristics and thickness were observed with a Stereo Microscope, Scanning Electron Microscopy (SEM) and a Sanfix Thickness Gauge. Based on the data obtained from this study, the optimal layer morphology is at a withdrawal speed of $2 \text{ mm}\cdot\text{s}^{-1}$ with a mass of HA as much as 12 g in suspension because it has a uniform thickness value according to the biomedical standards and a coated surface area of 91.8 %.

INTRODUCTION

Bone implants are used in cases of trauma, reconstructive implants that function as replacement damaged bone and joint structures and can restore function [1]. Implants that are widely used in orthopaedic surgery are Stainless steel (SS 316L), cobalt-chromium alloy (Co-Cr), pure titanium (Ti), and titanium alloys. Metal implants have major applications in load-bearing situations, such as hip and knee prostheses as well as for the fixation of internal and external fractures [1].

SS 316L has good corrosion resistance and is, therefore, widely used as a bone implant due to injuries, fractures or as a joint replacement and is cheaper than other metals such as $\text{Ti}_6\text{Al}_4\text{V}$ [2]. In addition to having good corrosion resistance, SS 316L also has strong, tough, ductile, and easy-to-clean surfaces. To increase the bioactivity and osteoconductivity of the metal, it is necessary to coat the implant material with Hydroxyapatite (HA) compounds [3]. Hydroxyapatite ($\text{Ca}_{10}(\text{PO}_4)_6(\text{OH})_2$) is the mineral form of calcium apatite. HA is a bio-ceramic material that has the potential as an implant material because it has the same components as bones and due to its biocompatibility [4-11]. There are several organic materials used to produce HA, such as bovine bones [12, 13], fish bones [14, 15], pig bones

[16], clam shells [17-20], egg shells [21, 22], snail shell [23], and others. The HA used in this study is derived from organic material that was derived from the bone scales of the white snapper. The utilisation of white snapper scales to be processed into natural HA can reduce waste that currently causes environmental pollution and can be of economic value. Natural HA from barramundi scales was used as a coating material for the implants, in addition natural HA has been used as a bone graft candidate [24].

Various methods that can be used for the HA coating process on metal surfaces are dip coating [25-27], electrophoretic deposition (EPD) [28-32], plasma spraying [33-35], and others. Dip coating is the easiest method to implement because the coating process is fast, can be carried out at low temperatures, is low cost and the coating results obtained are more uniform. Dip coating is perfect for coating rigid and flat substrates. This method also requires a smooth substrate surface and a low level of roughness. It is also suitable for SS 316L which has a smooth surface, so that it can produce a good coating quality. In the coating process that uses dip coating, the obtained results are influenced by several parameters such as the withdrawal speed, immersion time, suspension concentration and suspension viscosity [25].

The addition of a natural mass of HA in the coating suspension affects the coating on the SS 316L surface, namely the thickness of the layer and the obtained shear strength will increase. For the obtained coating to comply with biomedical application standards, it is necessary to experiment by varying the natural mass of HA in the coating suspension so that the resulting layer is not too thick and not too thin. In addition, this is undertaken because it has not been identified in detail how much natural mass of HA in the suspension produces a good coating quality. Likewise with the speed of withdrawal, when a higher speed of withdrawal is used, the thickness of the layer will decrease.

The used pulling speed refers to other studies where the speed that produces a good coating ranges from $2 - 4 \text{ mm}\cdot\text{s}^{-1}$. For the immersion time, 10 seconds was used, in accordance with previous studies, so that this condition is expected to support the possibility to obtain the maximum results later. Therefore, the research carried out in this study regarding the coating of hydroxyapatite on SS 316L uses the dip coating method by varying the natural mass of HA in the suspension at a withdrawal speed of $2 \text{ mm}\cdot\text{s}^{-1}$ and $4 \text{ mm}\cdot\text{s}^{-1}$ to obtain the optimal coating results.

EXPERIMENTAL

Sample Preparation

The sample used SS 316L in the form of a plate. The sample was cut using a hand grinder to obtain a sample size of $20 \text{ mm} \times 20 \text{ mm} \times 4 \text{ mm}$. After the SS 316L sample had been cut, a sanding process was carried out to smooth the surfaces and produce uniform quality on the surfaces of the specimen. Sanding is performed by using sandpaper with a mesh of 500, 800, and 1500 until the surface of the sample became even and flat. After sanding, polishing was carried out to smooth the surface of the sample using alumina powder.

The shiny sample was then washed using distilled water. At the time of washing with distilled water, there might still be a great deal of solid particles that are still attached to the sample, so that it can interfere with the coating process later. To overcome this, further cleaning was carried out using an ultrasonic machine. The cleaning process was carried out by immersing the sample using a 70 % ethanol solution for 30 minutes, then the sample was separated from the ethanol solution, then cleaned with distilled water, soaked in acetone for another 30 minutes. After that, the sample was separated from the acetone solution, which was then soaked using a 0.2 mol NaOH solution for 1 hour in the reaction gels. After that, the SS 316L sample was cleaned, then the sample was dried with a hot stirrer at a temperature of $50 \text{ }^\circ\text{C}$ for 5 minutes.

The process of preparing the solution suspension was carried out by preparing natural HA, Polyvinyl Alcohol (PVA), and Aquades. Next, the entire composition of the ingredients was weighed using a Shimadzu Analytical Balance digital scale. The natural HA used Lates Calcarifer scales. The solution was then prepared by dissolving 2 g of PVA into 50 g of distilled water at a temperature of $121 \text{ }^\circ\text{C}$ and homogenised for 1 hour at a speed of 300 rpm on a magnetic stirrer. The dissolved PVA serves as a binder for coating the hydroxyapatite on the substrate. After the solution is homogeneous, the homogenisation was carried out for 20 hours at a speed of 150 rpm using a magnetic stirrer. Then, a nitric acid solution (HNO_3) was added to obtain a solution with a good pH for the coating, namely pH 4. The HA is added slowly with a composition of 4 g, 8 g, and 12 g according to the test variation.

The specifications of the natural hydroxyapatite from Lates Calcarifer scales have an average particle size of $10 \text{ }\mu\text{m}$ with a non-synthetic purity of 99 %. The processing was carried out by a mild processing process in the form of a spherical powder. Lates Calcarifer scales contain up to 66 % calcium and up to 33 % phosphorus. The particle shape is spherical as can be seen in Figure 1.

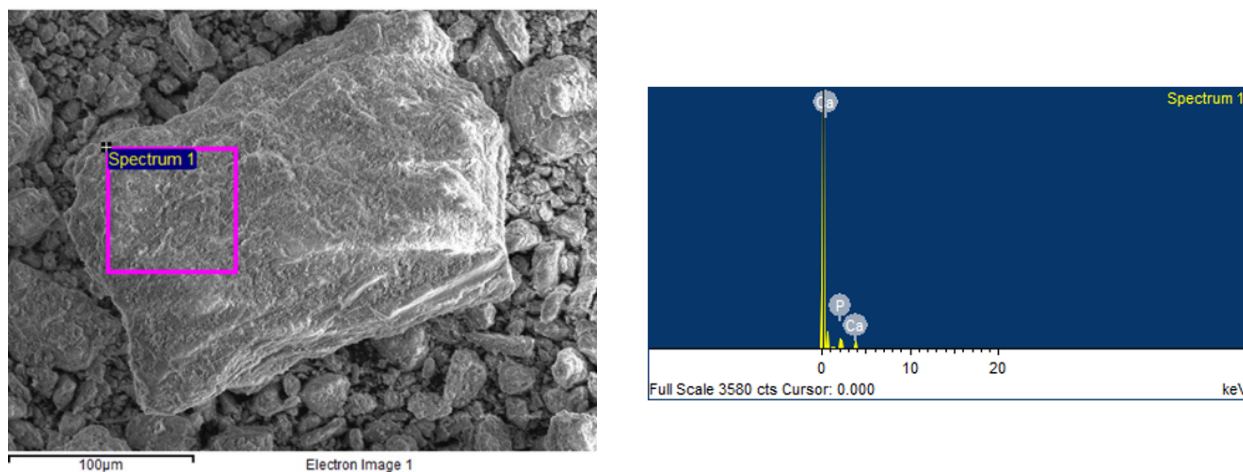


Figure 1. SEM and EDX results from natural hydroxyapatite processed lates calcarifer scales.

Coating SS 316L with the Dip Coating Method

The dip coating method was carried out after the SS 316L sample was made and the coating suspension was prepared. The sample is placed on a dip coating device which is then dyed with a constant drawing speed. The variations made to the withdrawal speed are $2 \text{ mm}\cdot\text{s}^{-1}$ and $4 \text{ mm}\cdot\text{s}^{-1}$. Then, the testing process was carried out by varying the speed of withdrawal and the mass of the used hydroxyapatite. After immersion, the samples were dried for 24 hours at room temperature.

Table 1. Experimental Variations.

Weight of Natural HA in Suspension (g)	Withdrawal Speed ($\text{mm}\cdot\text{s}^{-1}$)	Immersion Time (s)	Number of Sample
4	2	10	3
8			
12			
4	4	10	3
8			
12			

Sintering Process

The SS 316L sample, which was coated with hydroxyapatite, is then sintered to make the layer not easily brittle and detachable. The sintering process is carried out using a vacuum furnace which aims to increase the bond between the natural HA layer and the SS 316L surface to make it strong and not easily separable. A Ceramcofire S model vacuum furnace was used. The sintering process consists of heating to a temperature and holding it there so that there is an even temperature distribution in all parts of the sample, and then cooling at the furnace temperature (annealing). The sintering process was carried out at a temperature of $800 \text{ }^\circ\text{C}$ for 1 hour with a heating and cooling rate of $5 \text{ }^\circ\text{C}\cdot\text{min}^{-1}$.

Sample Characterisation

The surface morphology of the SS 316L samples was studied using an Olympus SZX10 LG-PS2 stereo microscope and a Hitachi Horiban S-3400 Scanning Electron Microscope (SEM). Observations were made to see the microstructure of the natural hydroxyapatite coating on the SS 316L samples. The thickness of the natural hydroxyapatite layer was controlled using a Sanfix GM-280 Thickness Gauge Series.

RESULTS AND DISCUSSION

Morphology of the HA Coating Result on the SS 316L Surface

Based on the research that has been undertaken, the HA coating on the SS 316L surface were observed using an Olympus SZX10 LG-PS2 stereo microscope with $1\times$ magnification and with SEM with $200\times$ magnification. The obtained results showed that there were differences in the surface characteristics of the SS 316L coated with natural HA without a natural HA coating. The results of the natural HA coating on SS 316L showed a colour change on the surface.

The results indicate that almost the entire SS 316L surface is coated with natural HA. The SS 316L material that is coated with natural HA has a white surface while the uncoated sample is dark grey. Figure 2a displays a sample with a withdrawal speed of $2 \text{ mm}\cdot\text{s}^{-1}$ with 4 g of natural HA. It is shown that the natural HA has not covered the entire surface, so that one can still distinguish between the SS 316L surface and the natural HA. Figure 2b shows a sample with a withdrawal speed of $4 \text{ mm}\cdot\text{s}^{-1}$ with 4 g of natural HA. In this sample, there is a natural accumulation of HA at the bottom of SS 316L so that the natural HA that coats the surface has not been distributed throughout the SS 316L surface. Figure 2c shows a sample with a withdrawal speed of $2 \text{ mm}\cdot\text{s}^{-1}$ with 8 g of natural HA. In the picture, the coating results are more evenly distributed than the previous sample and cover the entire SS 316L surface. Figure 2d shows a sample with a withdrawal speed of $4 \text{ mm}\cdot\text{s}^{-1}$ with 8 g of natural HA. In this section, it is almost the same as the previous sample, the entire surface has been evenly coated with natural HA, but the resulting layer is still thin like the previous sample. Figure 2e shows a sample with a withdrawal speed of $2 \text{ mm}\cdot\text{s}^{-1}$ with 12 g of natural HA. The coating results on this sample have been thoroughly and evenly distributed and cover the entire SS 316L surface and the formed layer is thicker than some of the previous samples. The last sample shown in Figure 2f is a sample with a withdrawal speed of $4 \text{ mm}\cdot\text{s}^{-1}$ with 12 g of natural HA. This section shows the coating results are evenly distributed over the entire SS 316L surface.

Based on the results of the observations of the morphology of the natural HA layer using a stereo microscope with $1\times$ magnification and SEM with $200\times$ magnification, the SS 316L surface was coated with natural HA. This observation showed that in the sample immersed with 12 g of natural HA in the suspension, the resulting layer was thicker and spread evenly over the entire surface compared to that of the 4 g and 8 g of natural HA. The results of the above study indicate that good coating results are obtained at a withdrawal speed of $2 \text{ mm}\cdot\text{s}^{-1}$ and 12 g of natural HA. This result is also confirmed by the variation in the natural mass of HA in the suspension at a draw speed of $4 \text{ mm}\cdot\text{s}^{-1}$ where a good layer is also present with 12 g of natural HA.

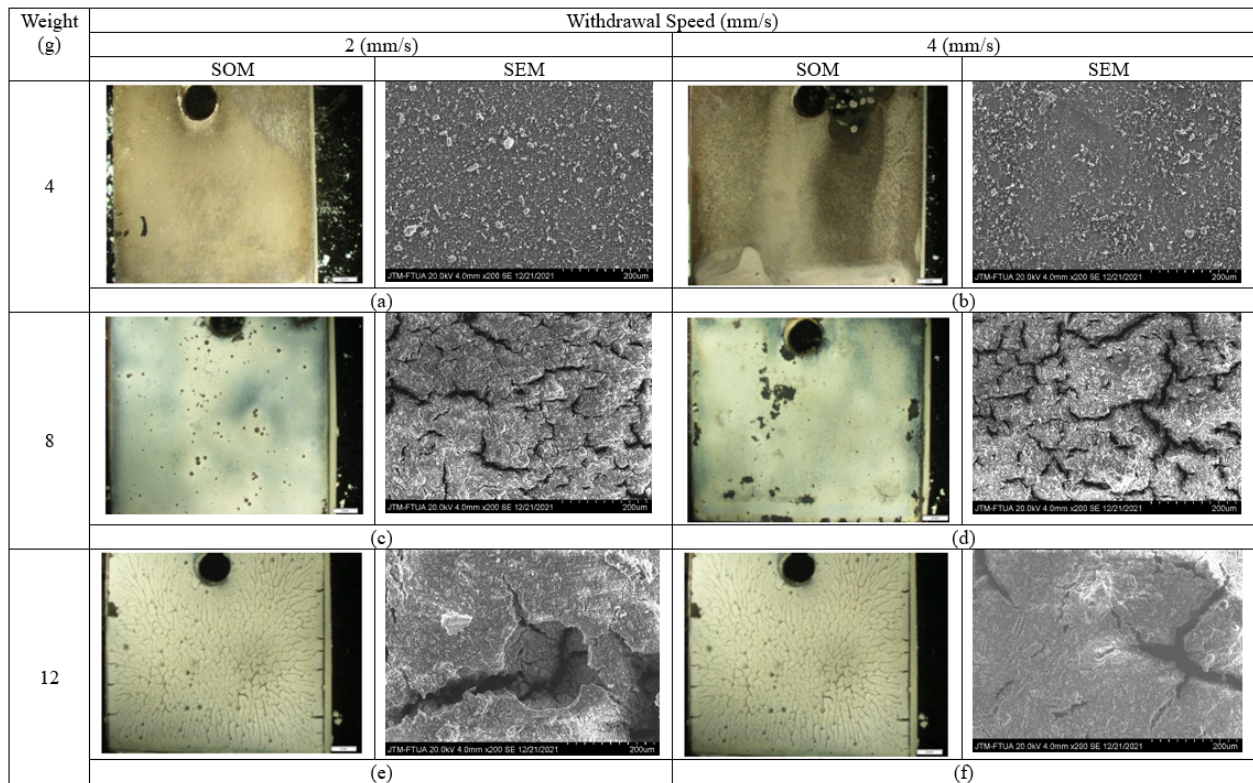


Figure 2. Observation of the morphology of HA coating on the surface of SS 316L which is influenced by variations in the speed of withdrawal and the weight of natural HA used by the dip coating method. SOM = Stereo Optical Microscope, SEM = Scanning Electron Microscope, (a) 2 mm·s⁻¹, 4 g natural HA (b) 4 mm·s⁻¹, 4 g natural HA (c) 2 mm·s⁻¹, 8 g natural HA (d) 4 mm·s⁻¹, 8 g natural HA (e) 2 mm·s⁻¹, 12 g natural HA (f) 4 mm·s⁻¹, 12 g natural HA.

At a withdrawal speed of 2 mm·s⁻¹ with each variation of the natural HA in the suspension of 4 g, 8 g, and 12 g, there is still a little imperfect agglomeration of natural HA particles, causing cracks. However, the variation of the natural mass of the HA with this speed showed more even results than the 4 mm·s⁻¹ withdrawal speed. These results indicate that the withdrawal speed of 2 mm·s⁻¹ can distribute natural HA particles better than the speed of 4 mm·s⁻¹. So that, in this condition, the difference in the results of the samples that have been immersed in each variation of natural HA dissolved in the coating suspension can be clearly seen.

The Effect of the Natural HA Mass in the Suspension used on the Surface Coverage on the Coating Surface

The results of the study showed that the variations in the natural mass of HA in the suspension layer at the withdrawal speed of 2 mm·s⁻¹ and 4 mm·s⁻¹ on the surface coverage of the SS 316L had an effect. The effect of these variations on the surface area of the HA layer on SS 316L can be seen in Figure 3.

Based on the graph of the average measurement results above, the highest percentage of surface coverage is at a withdrawal speed of 2 mm·s⁻¹ at 12 g of natural

HA. In this variation, the SS 316L coated surface area is 91.88 %. From the figure, there is a relationship between the speed of withdrawal and the surface coverage. At a withdrawal speed of 2 mm·s⁻¹, the percentage of the coated surface area is 91.88 % with a natural mass of 12 g of HA. Meanwhile, at a withdrawal speed of 4 mm·s⁻¹ with the same natural mass of HA, the percentage of the coated surface area was 90.08 %. The results of this test were also confirmed in the conditions of 4 g and 8 g of natural HA which showed a percentage of surface area

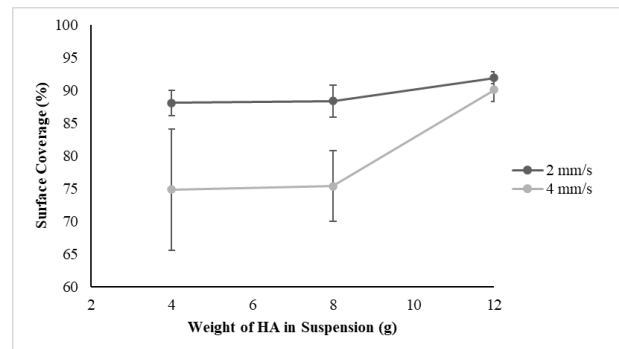


Figure 3. The relationship of weight variation of natural HA in suspension at 2 mm·s⁻¹ and 4 mm·s⁻¹ withdrawal speeds to the coating surface coverage.

coated with the same pattern at speeds of $2 \text{ mm}\cdot\text{s}^{-1}$ and $4 \text{ mm}\cdot\text{s}^{-1}$. Based on the measurement results above, the best percentage of the surface coverage is with the coating process with a withdrawal speed of $2 \text{ mm}\cdot\text{s}^{-1}$. This happens because the lower the withdrawal speed for the coating, the more natural HA sticks to the SS 316L surface which results in the entire surface being covered by natural HA so that the coated area will also increase. However, there are also differences in the percentage of the surface area coated on the natural mass of HA 4 g, 8 g and 12 g. In the suspension conditions by dissolving 4 g of natural HA, the percentage of the coated surface area was 90.08 % at a withdrawal speed of $4 \text{ mm}\cdot\text{s}^{-1}$. Meanwhile, in the natural mass of HA in which as much as 4 g and 8 g was dissolved, the percentage of the coated surface area was 75.73 % and 74.85 %, respectively, at the same withdrawal speed. So, based on Figure 4, the best percentage of the surface coverage is with the sample with a suspension of 12 g of the natural HA solution. In the results of the research [31] by coating TNTZ with HA using the EPD method with a voltage of 7 volts and a coating time of 5 minutes, the surface coverage value is 6.972 % and the thickness average is $51.73 \text{ }\mu\text{m}$.

The Effect of the Natural HA Mass in the used Suspension on the Thickness of the Natural HA Layer on SS 316L

In this study, the measurement of the coating thickness was carried out after the sintering process. The data from the measurement of the thickness of the hydroxyapatite layer on SS 316L on the variation of the natural mass of HA in the suspension used at withdrawal speeds of $2 \text{ mm}\cdot\text{s}^{-1}$ and $4 \text{ mm}\cdot\text{s}^{-1}$ can be seen in Figure 4.

In the graph above, the highest natural thickness of HA was found in the sample with a withdrawal speed of $2 \text{ mm}\cdot\text{s}^{-1}$ at 12 g of natural HA. The results in Figure 4 show that the average layer thickness values are in the range of 114 – 182 μm . In the results of the measurement of the thickness of the layer, there was a decrease in the thickness, although not too large with the increase in the

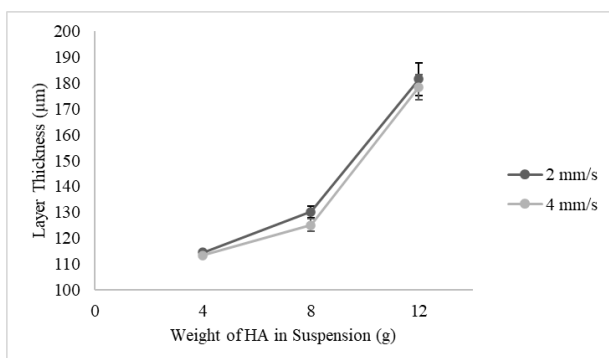


Figure 4. The relationship of weight variation of natural HA in suspension at withdrawal speeds of $2 \text{ mm}\cdot\text{s}^{-1}$ and $4 \text{ mm}\cdot\text{s}^{-1}$ to the thickness of the natural HA.

speed of withdrawal, while the increase in the natural mass of HA in the suspension resulted in a thickness that was directly proportional to each increase in the natural mass of HA. At a withdrawal speed of $2 \text{ mm}\cdot\text{s}^{-1}$, the thickness of the natural HA layer was 181.43 μm , 130.19 μm , and 114.51 μm . Meanwhile, at a draw speed of $4 \text{ mm}\cdot\text{s}^{-1}$, the natural thickness of HA obtained was 178.34 μm , 124.99 μm , and 113.38 μm . The reason for this is that the higher the withdrawal speed given, the contact that occurs between the SS 316L substrate and the suspension layer for deposition will be shorter which results in little natural HA sticking to the surface so that its thickness will decrease.

Furthermore, in Figure 4, in the three variations of the mass of hydroxyapatite used to make the suspension layer, different thickness values are also obtained. In the sample that was dipped in a layer suspension with 12 g of natural HA, the thickness value was 181.433 μm at a withdrawal speed of $2 \text{ mm}\cdot\text{s}^{-1}$. While the samples with the natural suspension of HA dissolved in as much as 8 g and 4 g at the same withdrawal speed had thickness values of 130.19 μm and 114,506 μm , respectively. Moreover, on coating the SS 316L sample with the natural suspension of HA dissolved in as much as 12 g at a withdrawal speed of $4 \text{ mm}\cdot\text{s}^{-1}$, a thickness value of 178.346 μm was obtained. At the same speed, but with a different natural mass of HA, namely 8 g and 4 g of HA, the layer thickness values were 124.993 μm and 113.383 μm . These results indicate that the sample, by dissolving 12 g of natural HA into the coating suspension, resulted in a higher layer thickness than the sample in the coating suspension by dissolving 4 g and 8 g of natural HA. This is because when more natural HA is used, the natural mass of HA deposited on the substrate surface will increase so that its thickness will increase. The layer thickness can affect the osteointegration of implants with bone tissue [36, 37].

Based on the data from the measurement of the thickness of the layer above, the obtained data are in accordance with the parameters required for biomedical applications. The thickness parameter required for the HA layer for biomedical applications, based on the research that has been carried out, is in the range of 50 – 200 μm [38].

Natural Mass Increase of HA in SS 316L

Measurement of the mass gain in SS 316L was carried out before and after the sample was coated with natural HA. The results of the measurements of the increase in the natural mass of HA in SS 316L to the variation of the natural mass of HA used in the suspension can be seen in Figure 5.

Based on Figure 5, at a withdrawal speed of $2 \text{ mm}\cdot\text{s}^{-1}$ by dissolving 12 g of natural HA, an increase in the layer mass of 74.53 mg occurs, while, at the same speed, but with natural variations of HA dissolved in 8 g and 4 g of the suspension, there was also an increase in the

mass, namely 15.43 mg and 3.23 mg, respectively. At a withdrawal speed of $4 \text{ mm} \cdot \text{s}^{-1}$ with the natural variation of HA dissolved in the layer suspension of 4 g, 8 g, and 12 g, there was also an increase in mass of 2.57 mg, 13.83 mg, and 66.4 mg, respectively. Based on the data above, the increase in the natural mass of HA can increase the mass of the 316L SS layer.

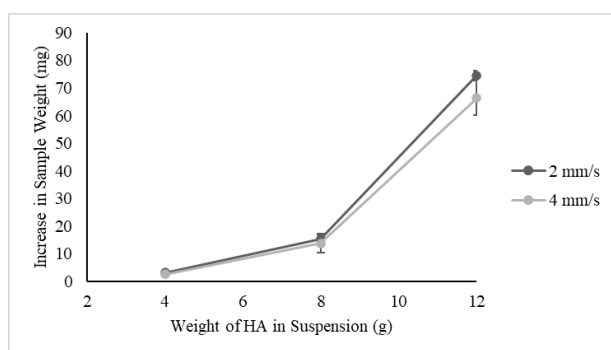


Figure 5. The relationship of the effect of the weight of natural HA in suspension at the withdrawal speed of $2 \text{ mm} \cdot \text{s}^{-1}$ and $4 \text{ mm} \cdot \text{s}^{-1}$ on the increase in sample weight.

CONCLUSIONS

The morphology of the natural HA coating on the SS 316L surface is influenced by the natural mass of HA dissolved in the coating suspension. The more natural HA dissolved in the suspension, the greater the percentage of the sample surface area coated by the natural HA. The natural mass of HA, as much as 12 g, at a withdrawal speed of $2 \text{ mm} \cdot \text{s}^{-1}$ resulted in a better and more even surface morphology compared to the natural mass of HA which was dissolved in as much as 4 g and 8 g in the suspension. This was confirmed in the experiments with a withdrawal speed of $4 \text{ mm} \cdot \text{s}^{-1}$ where the natural mass of HA dissolved in as much as 12 g also produced a good layer morphology on the surface compared to the 4 g and 8 g of natural HA dissolved in the suspension. The best morphology of the natural HA coating was found at a withdrawal speed of $2 \text{ mm} \cdot \text{s}^{-1}$ and 12 g of natural HA dissolved in the coating suspension with a surface coverage percentage of 91.8 %. Changes in the mass of the hydroxyapatite dissolved in the suspension also cause changes in the thickness of the layer and the mass of the sample. The more natural HA dissolved in the suspension, the thickness of the layer and the mass of the resulting sample will increase. The layer thickness obtained is in the range of 114 – 182 μm .

Acknowledgement

The authors would like to thank the Ministry of Education and Culture for providing PMDSU Scholarships and research budgets from DRTPM Dikti in 2022 and also publication support from engineering Faculty of Universitas Andalas.

REFERENCES

1. Mahyudin F., Widhiyanto L., Hermawan H. (2016): Biomaterials in orthopaedics. *Biomaterials and Medical Devices: A Perspective from an Emerging Country*, 161-181. doi: 10.1007/978-3-319-14845-8_7.
2. Saravanan I., Peruman A. E., Vettivel S. C., Selvakumar N., Baradeswaran A. (2015): Optimizing wear behavior of TiN coated SS 316L against Ti alloy using Response Surface Methodology. *Materials & Design*, 67, 469-482. doi: 10.1016/j.matdes.2014.10.051.
3. Arcos D., Vallet-Regi M. (2020): Substituted hydroxyapatite coatings of bone implants. *Journal of Materials Chemistry B*, 8(9), 1781-1800. doi: 10.1039/c9tb02710f.
4. Zhou H., Lee, J. (2011): Nanoscale hydroxyapatite particles for bone tissue engineering. *Acta biomaterialia*, 7(7), 2769-2781. doi: 10.1016/j.actbio.2011.03.019.
5. Kolmas J., Krukowski, S., Laskus A., Jurkitewicz M. (2016): Synthetic hydroxyapatite in pharmaceutical applications. *Ceramics International*, 42(2), 2472-2487. doi: 10.1016/j.ceramint.2015.10.048.
6. Esmaeili S., Akbari Aghdam H., Motififard M., Saber-Samandari, S., Montazeran A. H., Bigonah M., et al. (2020): A porous polymeric-hydroxyapatite scaffold used for femur fractures treatment: fabrication, analysis, and simulation. *European Journal of Orthopaedic Surgery & Traumatology*, 30, 123-131. doi: 10.1007/s00590-019-02530-3.
7. Sivaperumal V. R., Mani R., Nachiappan M. S., Arumugam K. (2017): Direct hydrothermal synthesis of hydroxyapatite/alumina nanocomposite. *Materials characterization*, 134, 416-421. doi: 10.1016/j.matchar.2017.11.016.
8. Szcześ A., Hołysz L., Chibowski E. (2017): Synthesis of hydroxyapatite for biomedical applications. *Advances in Colloid and Interface Science*, 249, 321-330. doi: 10.1016/j.cis.2017.04.007.
9. Catalgol Z. (2019): Sintering effect on borosilicate glass-bovine hydroxyapatite composites. *Journal of the Australian Ceramic Society*, 55, 1075-1079. doi: 10.1007/s41779-019-00320-y.
10. Fadli A., Yenti S. R., Prabowo A., Aledya S. P., Fadila R., Susanto R. (2021): The Synthesis of Hydroxyapatite Powder Using Shaker Mill Technique. *Journal of Southwest Jiaotong University*, 56(2), 22-23. doi: 10.35741/issn.0258-2724.56.2.3.
11. Zakaria S. M., Sharif Zein S. H., Othman M. R., Yang, F., Jansen J. A. (2013): Nanophase hydroxyapatite as a biomaterial in advanced hard tissue engineering: a review. *Tissue Engineering Part B: Reviews*, 19(5), 431-441. doi: 10.1089/ten.teb.2012.0624.
12. Yuliana R., Rahim E. A., Hardi J. (2017): Sintesis hidroksiapatit dari tulang sapi dengan metode basah pada berbagai waktu pengadukan dan suhu sintering. *KOVALEN: Jurnal Riset Kimia*, 3(3), 201-210.

13. Barakat N. A., Khil M. S., Omran, A. M., Sheikh F. A., Kim H. Y. (2009)-, Extraction of pure natural hydroxyapatite from the bovine bones bio waste by three different methods. *Journal of Materials Processing Technology*, 209(7), 3408-3415. doi: 10.1016/j.matprotec.2008.07.040.
14. Pal A., Paul S., Choudhury A. R., Balla V. K., Das M., Sinha A. (2017): Synthesis of hydroxyapatite from Lates Calcarifer fish bone for biomedical applications. *Materials Letters*, 203, 89-92. doi: 10.1016/j.matlet.2017.05.103.
15. Anggresani L. (2020): Pengaruh waktu sintering terhadap hidroksiapatit berpori tulang ikan tenggiri dengan proses sol-gel. *Chempublish Journal*, 5(1), 46-56. doi: 10.22437/chp.v5i1.8686.
16. Ofudje E. A., Rajendran A., Adeogun A. I., Idowu M. A., Kareem S. O., Pattanayak D. K. (2018): Synthesis of organic derived hydroxyapatite scaffold from pig bone waste for tissue engineering applications. *Advanced Powder Technology*, 29(1), 1-8. doi: 10.1016/j.apt.2017.09.008.
17. Suci I. A., Ngapa Y. D. (2020). Sintesis dan Karakterisasi Hidroksiapatit (HAp) dari Cangkang Kerang Ale-Ale Menggunakan Metode Presipitasi Double Stirring. *CAKRA KIMIA (Indonesian E-Journal of Applied Chemistry)*, 8(2), 73-81.
18. Wati S. A. (2014). *Sintesis dan Karakterisasi Hidroksiapatit dari Limbah Cangkang Kerang Bulu (Anadara antiquata)* (Doctoral dissertation, Universitas Sumatera Utara).
19. Fadhilah R., Kurniawan R. A., Icha M. M. (2015): Sintesis Hidroksiapatit dari Cangkang Kerang Ale-Ale (*Meretrix Spp*) Sebagai Material Graft Tulang. *Jurnal Buletin Al-Ribaath*, 12(1), 44-60. doi: 10.29406/br.v12i1.79
20. Affandi A., Amri A., Zultiniar Z. (2015): Sintesis Hidroksiapatit Dari Cangkang Kerang Darah (*Anadara granosa*) dengan Proses Hidrotermal Variasi Rasio Mol Ca/P dan Suhu Sintesis. *Jurnal Online Mahasiswa (JOM) Bidang Teknik dan Sains*, 2(1), 1-8.
21. Malau N. D., Adinugraha, F. (2020): Penentuan suhu kalsinasi optimum CaO dari cangkang telur bebek dan cangkang telur burung puyuh. *Jurnal EduMatSains*, 4(2), 193-202.
22. Wardani N. S., Fadli A., Irdoni I. (2015): Sintesis Hidroksiapatit dari Cangkang Telur dengan Metode Presipitasi. *Jurnal Online Mahasiswa (JOM) Bidang Teknik dan Sains*, 2(1), 1-6.
23. Ahmed H. Y., Safwat N., Shehata R., Althubaiti E. H., Kareem S., Atef A., et al. (2022)? Synthesis of natural nano-hydroxyapatite from snail shells and its biological activity: antimicrobial, antibiofilm, and biocompatibility. *Membranes*, 12(4), 408. doi: 10.3390/MEMBRANES12040408.
24. Souliissa A. G., Nathania I. (2018): The efficacy of fish scales as bone graft alternative materials. *Scientific Dental Journal*, 2(1), 9-17.
25. Tang X., Yan X. (2017): Dip-coating for fibrous materials: Mechanism, methods and applications. *Journal of Sol-Gel Science and Technology*, 81, 378-404. doi: 10.1007/s10971-016-4197-7.
26. Aksakal B., Hanyaloglu C. (2008): Bioceramic dip-coating on Ti-6Al-4V and 316L SS implant Materials. *Journal of Materials Science: Materials in Medicine*, 19, 2097-2104. doi: 10.1007/s10856-007-3304-2.
27. Strobel C., Kadow-Romacker A., Witascheck T., Schmidmaier G., Wildemann B. (2011): Evaluation of process parameter of an automated dip-coating. *Materials Letters*, 65(23-24), 3621-3624. doi: 10.1016/j.matlet.2011.07.102.
28. Juliadmi D., Nuswantoro N. F., Fajri H., Indriyani I. Y., Affi J., Manjas M., et al. (2020): The coating of bovine-source hydroxyapatite on titanium alloy (Ti-6Al-4V ELI) using electrophoretic deposition for biomedical application. In *Materials Science Forum* (Vol. 1000, pp. 97-106). Trans Tech Publications Ltd. doi: 10.4028/www.scientific.net/MSF.1000.97.
29. Fajri H., Ramadhan F., Nuswantoro N. F., Juliadmi D., Tjong D. H., Manjas M et al. (2020): Electrophoretic deposition (EPD) of natural hydroxyapatite coatings on titanium Ti-29Nb-13Ta-4.6Zr substrates for implant material. In *Materials Science Forum* (Vol. 1000, pp. 123-131). Trans Tech Publications Ltd. doi: 10.4028/www.scientific.net/MSF.1000.123.
30. Nuswantoro N. F., Maulana I., Tjong D. H., Manjas M., Gunawarman G. (2018): Hydroxyapatite Coating on New Type Titanium, TNTZ, Using Electrophoretic Deposition. *Journal of Ocean, Mechanical and Aerospace-science and engineering-*, 56(1), 1-4.[Online]. Available: www.isomase.org
31. Nuswantoro N. F., Manjas M., Suharti N., Juliadmi D., Fajri H., Tjong D. H., et al. (2021): Hydroxyapatite coating on titanium alloy TNTZ for increasing osseointegration and reducing inflammatory response in vivo on Rattus norvegicus Wistar rats. *Ceramics International*, 47(11), 16094-16100. doi: 10.1016/j.ceramint.2021.02.184.
32. Nuswantoro N. F., Budiman I., Septiawarman A., Tjong D. H., Manjas M. (2019): Effect of applied voltage and coating time on nano hydroxyapatite coating on titanium alloy Ti₆Al₄V using electrophoretic deposition for orthopaedic implant application. In IOP Conference Series: *Materials Science and Engineering* (Vol. 547, No. 1, p. 012004). IOP Publishing. doi: 10.1088/1757-899X/547/1/012004.
33. Vardelle A., Moreau C., Themelis, N. J., Chazelas C. (2015): A perspective on plasma spray technology. *Plasma Chemistry and Plasma Processing*, 35, 491-509. doi: 10.1007/s11090-014-9600-y.
34. Odhiambo J. G., Li W., Zhao Y., Li C. (2019): Porosity and its significance in plasma-sprayed coatings. *Coatings*, 9(7), 460. doi: 10.3390/coatings9070460.
35. Singh A., Singh G., Chawla V. (2018): Characterization and mechanical behaviour of reinforced hydroxyapatite coatings deposited by vacuum plasma spray on SS-316L alloy. *Journal of the Mechanical Behavior of Biomedical Materials*, 79, 273-282. doi: 10.1016/j.jmbbm.2018.01.005.
36. Svehla M., Morberg P., Bruce W., Zicat B., Walsh W. R. (2002): The effect of substrate roughness and hydroxyapatite coating thickness on implant shear strength. *The Journal of Arthroplasty*, 17(3), 304-311. doi: 10.1054/arth.2002.30410.
37. Lynn, A. K., & DuQuesnay, D. L. (2002). Hydroxyapatite-coated Ti-6Al-4V: Part 1: the effect of coating thickness on mechanical fatigue behaviour. *Biomaterials*, 23(9), 1937-1946. doi: 10.1016/S0142-9612(01)00321-0
38. Heimann R. B. (2002). Materials science of crystalline bioceramics: a review of basic properties and applications. *CMU J*, 1(1), 23-46.